THE JOURNAL OF PHYSICAL CHEMISTRY B

Article

Cite This: J. Phys. Chem. B 2019, 123, 5805−5813

pubs.acs.org/JPCB

Theoretical Analysis of Run Length Distributions for Coupled Motor Proteins

Qian Wang[†] and Anatoly B. Kolomeisky*[,†,‡,¶,§]

[†]Center for Theoretical Biological Physics, [‡]Department of Chemistry, [¶]Department of Chemical and Biomolecular Engineering, and [§]Department of Physics and Astronomy, Rice University, Houston, Texas 77005, United States

ABSTRACT: Motor proteins, also known as biological molecular motors, play important roles in various biological processes. In recent years, properties of single-motor proteins have been intensively investigated using multiple experimental and theoretical tools. However, in real cellular systems biological motors typically function in groups, but the mechanisms of their collective dynamics remain not well understood. Here we investigate theoretically distributions of run lengths for coupled motor proteins that move along linear tracks. Our approach utilizes a method of first-passage processes, which is supplemented by Monte Carlo computer simulations. Theoretical analysis allowed us to clarify several aspects of the cooperativity mechanisms for coupled biological molecular motors. It is found that the run length distribution for two motors, in contrast to single motors, is nonmonotonic. In addition, the transport efficiency of two-motor complexes might be strongly increased. We also argue that the degree of cooperativity is influenced by several characteristics of motor proteins such as the strength of intermolecular interactions, stall forces, dissociations constants, and the detachment forces. The application of our theoretical analysis for several motor proteins is also discussed.

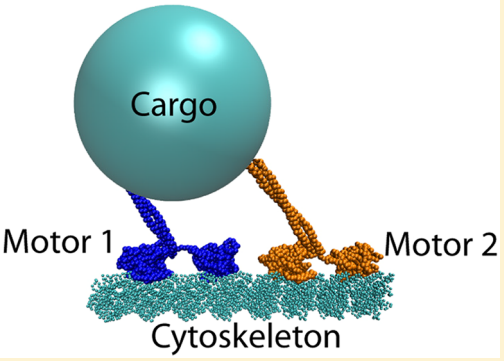

INTRODUCTION

Motor proteins, also called biological molecular motors, correspond to several classes of active enzymatic molecules that are crucial for successful functioning of cellular systems.[1−4] They support most major biological processes, including transfer and maintaining of genetic information, muscles functioning, cell division, intracellular transport, and cell motility.[1−7] Malfunctioning of motor proteins frequently leads to serious diseases, including cancer and various neurodegenerative disorders.[8,9] It is known that motor proteins move along linear filaments, such as microtubules, actin filaments, or nucleic acids, and catalyze exothermic chemical reactions, such as the hydrolysis of adenosine triphosphate (ATP) or biopolymerization.[4,10] Molecular motors are able to convert a fraction of the released chemical energy into mechanical work that is necessary for their functions.[1,2,4]

Because of their important roles in cellular processes, motor proteins have been widely investigated using a variety of experimental and theoretical methods.[3,4,6,7,11] With recent advances in single-molecule experimental techniques, the properties of single-motor proteins have been quantified with high temporal and spatial resolutions.[4,11] Motor proteins transporting cellular cargoes along linear protein filaments have been classified as nonprocessive and processive, depending on the strength of their interactions with linear tracks.[4] After associating to linear filaments, nonprocessive motors walk relatively short distances before detaching. At the same time, processive motors can walk longer distances. To quantify the degree of processivity, run lengths distributions for various motor proteins have been precisely measured by several groups.[12,13] This provided crucial information on the mechanisms of biological molecular motors because the run length distributions of single-motor proteins have been also theoretically evaluated recently.[14,15]

Although properties of single-motor proteins are important for understanding biological transport phenomena,[4] in real biological systems motor proteins typically work in teams that might include many motor species.[4,7,16,17] However, the mechanisms of collective behavior of biological motors remain not well understood.[4,7,16,18] One of the barriers to measure the properties of multiple-motor proteins using single-molecule experimental techniques is to control the actual number of motors participating in the transport and their binding positions on the cargo. As a result, controversial experimental observations on collective dynamic properties of multiple-motor proteins have been reported.[16,19,20] Although the issue of precise determination of number of participating motors has been partially solved by employing the engineered DNA scaffolds,[21,22] only few dynamic properties of motor proteins assemblies have been reliably measured so far.[16] The distributions of run lengths of coupled motor proteins have not been measured yet, although the average run lengths have been reported.[16] But the main problem for understanding the collective dynamics of motor proteins is a lack of theoretical

Received: May 17, 2019
Revised: June 16, 2019
Published: June 18, 2019

DOI: 10.1021/acs.jpcb.9b04710
J. Phys. Chem. B 2019, 123, 5805−5813

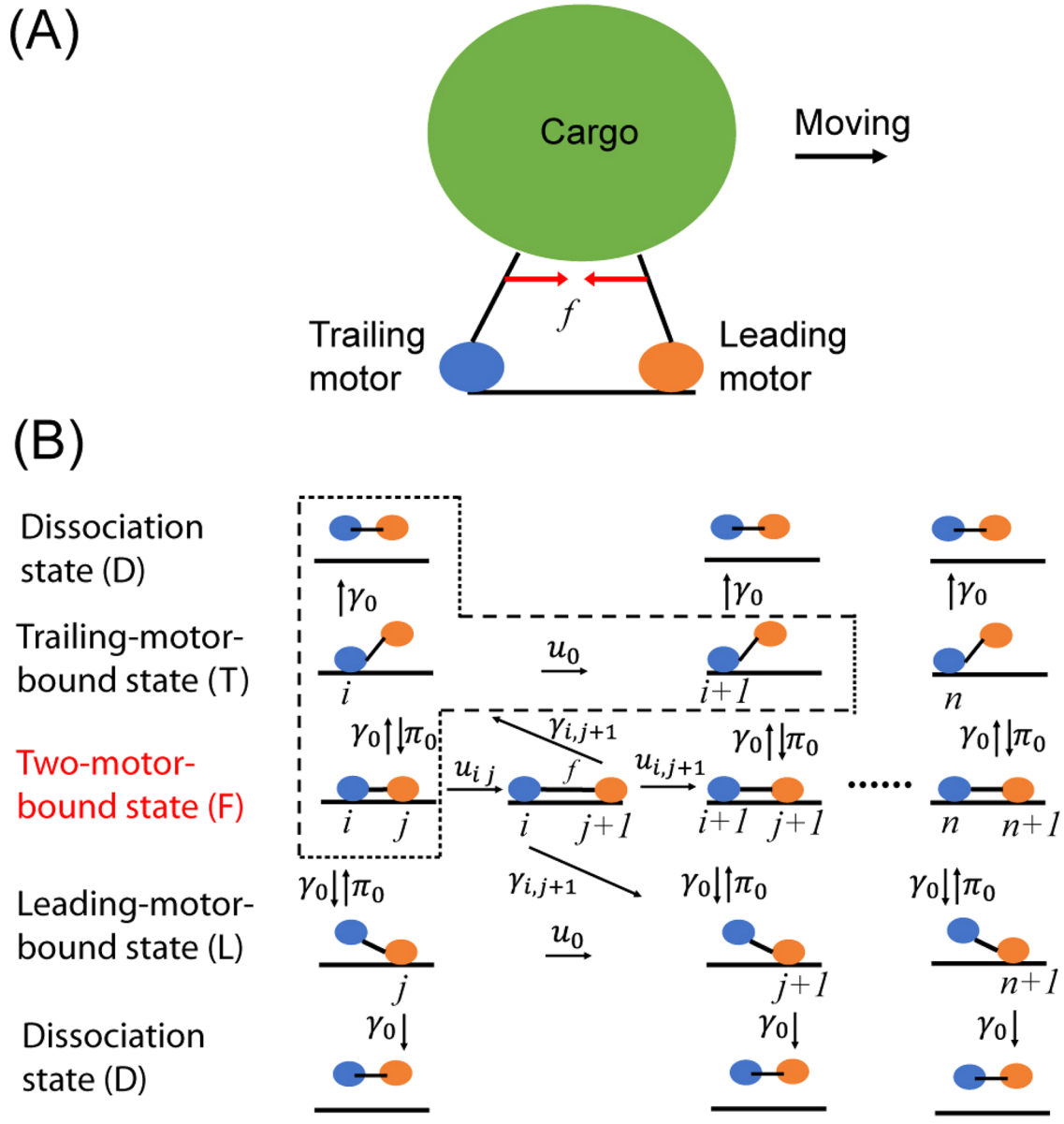

Figure 1. (A) Schematic illustration of the cellular cargo motion transported by two motor proteins. When the distance between the two motor proteins increases, the tension between them increases too. This effect is modeled as an elastic spring between two motors. (B) Chemical kinetic scheme for the system with two interacting molecular motors walking along the linear track. Orange circles describe the leading motor, while blue circles describe the trailing motor in two-motor-bound states. The process described in eq 5 is highlighted by the dashed box in order to explain better the method of backward master equations.

methods that would quantitatively describe the distributions of dynamic properties of motors and connect them with underlying molecular properties.

Theoretical tools are crucial for our efforts to clarify the molecular mechanisms of motor proteins transport.[4,16,18,23,24] The run length distributions of single motors has been recently explicitly calculated under an assumption of infinite linear tracks.[14] A more general theoretical framework to evaluate the run lengths distributions at different and more realistic conditions, such as the finite length of tracks and the presence of intermediate chemical states, has been also presented.[15] Nevertheless, there are no explicit theoretical analyses on the run length distributions of several coupled motor proteins. Noticeably, the transport by two motors has been investigated in several previous theoretical studies, but the coupling between the two motors was neglected, or only qualitative arguments about the run length distribution were given.[25,26]

In order to fill a theoretical gap, in this paper, we develop a new theoretical approach to quantify the transport of two coupled motor proteins. Using the method of first-passage processes that was successful in describing single motors,[4] the run lengths distributions for two coupled motor proteins are explicitly evaluated. Our theoretical results, which are supported by extensive Monte Carlo simulations, allow us to quantify the efficiency and the cooperativity in the motor proteins transport. The application of this theoretical analysis for several real motor proteins is also discussed.

THEORY

Run Length Distributions for Two Coupled Motor Proteins. Let us consider a system of two coupled motor

DOI: 10.1021/acs.jpcb.9b04710
J. Phys. Chem. B 2019, 123, 5805−5813

proteins moving along infinite linear track, as illustrated in Figure 1. This linear track might, for example, represent a protein filament (microtubules or actin filaments), or it might correspond to nucleic acids (DNA and RNA molecules). Assuming that the motor proteins complex moves preferentially in one direction, one can identify leading and trailing motors (see Figure 1A). If the leading motor is at the site j while the trailing motor is at the site i, this state of the system is denoted as (i, j). It is assumed that two motors interact with each other, and the interaction potential is modeled as an elastic spring with a spring constant k. Therefore, for any two-motors-bound state (i, j), the intermotor tension, f, can be represented as

$$f = kd(j - i - l_0) \tag{1}$$

where d is the motor step size, which is equal to the distance between 2 neighboring lattice sites (Figure 1), and l_0 represents the site separation between the two motors in the equilibrated state ($f = 0$). For convenience, we set $l_0 = 1$.

We assume that the system starts from a two-motors-bound state $(0, 1)$. Each motor can walk forward from the state (i, j) (if the forward site is available) with an interaction-dependent rate u_{ij}, or it can unbind from the linear filament with an interaction-dependent dissociation rate γ_{ij}; see Figure 1B. To simplify calculations, we neglected the possibility of backward steps because for most motor proteins the forward rate is orders of magnitude higher than the backward rate in the absence of external forces, and we consider here mostly the dynamic and not energetic aspects of the motor proteins motion.[4,27,28] One should notice that biological molecular motors are functioning in cells under nonequilibrium conditions when the detailed balance is always broken. Thus, this is a reasonably safe approximation, which is needed in order to obtain an analytical solution. The stepping of the leading motor corresponds to a transition from the state (i, j) to $(i, j + 1)$, and the corresponding stepping rate depends on the interaction as

$$u_{ij} = u_0(1 - \langle f \rangle / F_s) = u_0[1 - (kd(j - i - 0.5)]/F_s) \tag{2}$$

where u_0 is the forward rate in the absence of interactions, $\langle f \rangle$ is the average tension between two motors, and F_s is the stalling force, which corresponds to the interaction that prohibits the transition. Please note that the factor 0.5 in eq 2 comes from the following arguments. The stepping of the leading motor corresponds to a transition from the state (i, j) to $(i, j + 1)$. During this stepping process the intermotor tension f is not constant but gradually increasing from $kd(j - i - 1)$ to $kd(j - i)$. For convenience, we choose here the average value of f, $\langle f \rangle = \frac{kd(j - i - 1) + kd(j - i)}{2} = kd(j - i - 0.5)$. It should be noted also that the dependence of the stepping rate on the tension is a complex function, but here we make an assumption that this dependence is a linear function of the force. Although this is clearly a strong oversimplification,[4,6] it is expected that this should not affect much the main physical predictions of the model.

The stepping of the trailing motor shifts the system from the state (i, j) to $(i + 1, j)$. In order again to simplify calculations, here we postulate that for the trailing motor the stepping rate is independent of intermolecular interaction, $u_{ij}(f) = u_0$. This is based on observations for several cytoskeletal motor proteins indicating that the velocity of the motor is barely increased by the assisting forces.[29,30] The trailing motor is experiencing the assisting force from the leading motor. In addition, we take into account the fact that the trailing motor cannot pass the leading one. Therefore, if $j - i = 1$, the forward stepping of the trailing motor is prohibited. It is also assumed that leading and trailing motors alternate their steps. This means that the distance between two motors can be only one or two sites, and other conformations with larger distances between the motors are not allowed; see Figure 1B.

In the two-motors-bound state (i, j), the unbinding of the motor from the site j leads to a single-motor-bound state i. The corresponding dissociation rate is given by

$$\gamma_{ij} = \gamma_0 e^{f/F_d} = \gamma_0 e^{kd(j-i-1)/F_d} \tag{3}$$

where γ_0 is the dissociation rate in the absence of intermotor tension and F_d is a characteristic force, which is called a detachment force. It quantifies the strength of interaction between the motor and the linear filament: the stronger the interactions, the larger is F_d. In the single-motor-bound state i, the system can move forward to the state $i + 1$ if the bound motor steps with a rate u_0, or it can return to the equilibrated two-motors-bound state ($|j - i| = l_0$) if the unbound motor rebinds to the track with a rate π_0; see Figure 1B. In addition, the single-bound motor can completely dissociate from the linear filament with a rate γ_0 (Figure 1B).

To obtain the explicit description of the run length distributions for the model of coupled two motors, as illustrated in Figure 1, a theoretical approach that was successful for describing the run length distributions of single motors is adopted.[15] We introduce a first-passage probability density function $F_{ij}(t)$, which is defined as a probability for the system to detach at some specific site n at time t if the initial state at time 0 is a two-motors-bound state (i, j). This meaning of the last state n before the dissociation is the following. It is the last state of the system before complete dissociation into the solution. It might happen either when the trailing motor sits on the site n and the leading motor is unbound or when the trailing motor is unbound and the leading motor sits on the site $n + 1$ (see Figure 1B). Then the probability of having a run length $l = nd$ can be calculated as

$$P(l) = \int_0^\infty F_{01}(t)\mathrm{d}t \tag{4}$$

This indicates that the starting position for the system is the state $(0, 1)$, and the complex of two coupled motors will make n steps before the complete dissociation from the track. We also introduce two more additional first-passage probability density functions, $L_i(t)$ and $T_i(t)$. $L_i(t)$ represents the probability of the motor complex to detach at the site n at time t if at time 0 the trailing motor is unbound and the leading motor is bound at the site i. Similarly, $T_i(t)$ is defined as the probability of the motor complex to detach at the site n at time t if at time 0 the leading motor is unbound and the trailing motor is bound at the site i.

The temporal evolution of the first-passage probability density functions is controlled by backward master equations:[4,15]

$$\frac{\mathrm{d}T_i(t)}{\mathrm{d}t} = u_0 T_{i+1}(t) + \pi_0 F_{i,i+1}(t) + \gamma_0 D_i(t) - (u_0 + \pi_0 + \gamma_0) T_i(t) \tag{5}$$

This equation describes the process in the kinetic scheme, which is shown in the dashed box in Figure 1B, meaning that in order to evolve from the state $T_i(t)$ to the final dissociation state, the system first needs to visit one the neighboring states of $T_i(t)$, i.e., $T_{i+1}(t)$, $F_{i,i+1}$, or $D_i(t)$. More explanations of the backward master equations and first-passage probabilities can be found in ref 4. Similarly, we can write the temporal evolution for other states:

DOI: 10.1021/acs.jpcb.9b04710
J. Phys. Chem. B 2019, 123, 5805−5813

$$\frac{dL_{i+1}(t)}{dt} = u_0 L_{i+2}(t) + \pi_0 F_{i,i+1}(t) + \gamma_0 D_i(t) - (u_0 + \pi_0 + \gamma_0) L_{i+1}(t) \quad (6)$$

$$\frac{dF_{i,i+1}(t)}{dt} = u_{i,i+1} F_{i,i+2}(t) + \gamma_{i,i+1}[T_i(t) + L_{i+1}(t)] - [u_{i,i+1} + 2\gamma_{i,i+1}] F_{i,i+1}(t) \quad (7)$$

$$\frac{dF_{i,i+2}(t)}{dt} = u_0 F_{i+1,i+2}(t) + \gamma_{i,i+2}[T_i(t) + L_{i+2}(t)] - [u_0 + 2\gamma_{i,i+2}] F_{i,i+2}(t) \quad (8)$$

Here, we assumed that the leading and the trailing motor walk alternately. This assumption will be justified in the following sections. In these equations we also introduced auxiliary functions $D_i(t)$, which reflect the boundary condition

$$D_i(t) = \begin{cases} \delta(t) & i = n \\ 0 & i \neq n \end{cases} \quad (9)$$

Equations 5, 6, 7, and 8 can be solved by utilizing Laplace transformations

$$\widetilde{F_{ij}}(s) = \int_0^\infty F_{ij}(t) e^{-st} dt \quad (10)$$

$$\widetilde{X_i}(s) = \int_0^\infty X_i(t) e^{-st} dt \quad (X = L, T) \quad (11)$$

$$\widetilde{D_i}(s) = \begin{cases} 1 & i = n \\ 0 & i \neq n \end{cases} \quad (12)$$

Then the backward master equations are modified into a set of algebraic equations:

$$(u_0 + \pi_0 + \gamma_0 + s)\widetilde{T_i}(s) = u_0 \widetilde{T_{i+1}}(s) + \pi_0 \widetilde{F_{i,i+1}}(s) + \gamma_0 \widetilde{D_i}(s) \quad (13)$$

$$(u_0 + \pi_0 + \gamma_0 + s)\widetilde{L_{i+1}}(s) = u_0 \widetilde{L_{i+2}}(s) + \pi_0 \widetilde{F_{i,i+1}}(s) + \gamma_0 \widetilde{D_i}(s) \quad (14)$$

$$\left[u_0\left(1 - \frac{kd}{2F_s}\right) + 2\gamma_0 + s\right] \widetilde{F_{i,i+1}}(s) = u_0\left(1 - \frac{kd}{2F_s}\right) \widetilde{F_{i,i+2}}(s) + \gamma_0[\widetilde{T_i}(s) + \widetilde{L_{i+1}}(s)] \quad (15)$$

$$[u_0 + 2\gamma_0 e^{kd/F_d} + s] \widetilde{F_{i,i+2}}(s) = u_0 \widetilde{F_{i+1,i+2}}(s) + \gamma_0 e^{kd/F_d}[\widetilde{T_i}(s) + \widetilde{L_{i+2}}(s)] \quad (16)$$

From these equations we obtain

$$\widetilde{F_{i,i+1}}(s) = \frac{(u_0 + \pi_0 + \gamma_0 + s)\widetilde{T_i}(s) - u_0 \widetilde{T_{i+1}}(s) - \gamma_0 \widetilde{D_i}(s)}{\pi_0} \quad (17)$$

$$A\widetilde{T_{i+2}}(s) - B\widetilde{T_{i+1}}(s) + C\widetilde{T_i}(s) = \frac{\gamma_0\left[s + u_0\left(1 - \frac{kd}{2F_s}\right) + 2\gamma_0\right]}{\pi_0} \widetilde{D_i}(s) - \frac{\gamma_0 u_0^2\left(1 - \frac{kd}{2F_s}\right)}{\pi_0(s + u_0 + 2\gamma_0 e^{kd/F_d})} \widetilde{D_{i+1}}(s) \quad (18)$$

where coefficients A, B, and C are given by

$$A = \frac{u_0^3\left(1 - \frac{kd}{2F_s}\right)}{\pi_0(s + u_0 + 2\gamma_0 e^{kd/F_d})} \quad (19)$$

$$B = \left\{u_0\left[s + u_0\left(1 - \frac{kd}{2F_s}\right) + 2\gamma_0\right](s + u_0 + 2\gamma_0 e^{kd/F_d}) + u_0^2\left(1 - \frac{kd}{2F_s}\right)(s + u_0 + \gamma_0 + \pi_0)\right\} / \{\pi_0(s + u_0 + 2\gamma_0 e^{kd/F_d})\} + \left\{u_0\gamma_0\pi_0\left(1 - \frac{kd}{2F_s}\right)e^{kd/F_d}\right\} / \{\pi_0(s + u_0 + 2\gamma_0 e^{kd/F_d})\} \quad (20)$$

and

$$C = \frac{\left[s + u_0\left(1 - \frac{kd}{2F_s}\right) + 2\gamma_0\right](s + u_0 + \pi_0 + \gamma_0)}{\pi_0} - \frac{u_0\gamma_0\left(1 - \frac{kd}{2F_s}\right)e^{kd/F_d})}{(s + u_0 + 2\gamma_0 e^{kd/F_d})} - 2\gamma_0 \quad (21)$$

When $i \neq n$ or $i \neq n - 1$, using eq 12 one can easily show that the expression in eq 18 can be simplified into

$$A\widetilde{T_{i+2}}(s) - B\widetilde{T_{i+1}}(s) + C\widetilde{T_i}(s) = 0 \quad (22)$$

This suggests that the solution for the probability density function $\widetilde{T_i}(s)$ is of the form $\widetilde{T_i}(s) \sim x^i$, which after substituting into eq 22 yields

$$Ax^2 - Bx + C = 0 \quad (23)$$

with two roots

$$x_{1,2} = \frac{B \pm \sqrt{(B^2 - 4AC)}}{2A} \quad (24)$$

Therefore, the general solution for $\widetilde{T_i}(s)$ can be written as

$$T_i(s) = ax_1^i + bx_2^i \quad (25)$$

where a and b are unknown coefficients, which can be determined from boundary conditions at $i = n$ and $i = n - 1$. Applying these boundary conditions leads to

$$ax_1^n + bx_2^n = \frac{\gamma_0\left[s + u_0\left(1 - \frac{kd}{2F_s}\right) + 2\gamma_0\right]}{\pi_0 C} \quad (26)$$

$$-B(ax_1^n + bx_2^n) + C(ax_1^{n-1} + bx_2^{n-1}) = -\frac{\gamma_0 u_0^2\left(1 - \frac{kd}{2F_s}\right)}{\pi_0(s + u_0 + 2\gamma_0 e^{kd/F_d})} \quad (27)$$

Now we can evaluate the run length distribution for two coupled motor proteins by rewriting it in the following form

$$P(l) = \widetilde{F_{01}}(s = 0) \quad (28)$$

DOI: 10.1021/acs.jpcb.9b04710
J. Phys. Chem. B 2019, 123, 5805−5813

Using eq 17 we derive

$$P(l) = \frac{(u_0 + \pi_0 + \gamma_0)\widetilde{T}_0(s=0) - u_0\widetilde{T}_1(s=0)}{\pi_0} \tag{29}$$

Substituting eqs 25, 26, and 27 into eq 29, we obtain the final explicit expression for the run length distribution of the two-motor system:

$$P(l) = -\theta(x_1')^{-l/d} + \phi(x_2')^{-l/d} \tag{30}$$

In this equation, parameters θ, ϕ, x_1', and x_2' are positive coefficients (θ, $\phi > 0$; $x_1' > x_2' > 1$). They are found from the following equations

$$\theta = \frac{u_0 + \pi_0 + \gamma_0 - u_0 x_1'}{\pi_0\sqrt{B'^2 - 4A'C'}}\left[\frac{\gamma_0\left[u_0\left(1 - \frac{kd}{2F_s}\right) + 2\gamma_0\right]}{\pi_0 x_1'} - \frac{\gamma_0 u_0^2\left(1 - \frac{kd}{2F_s}\right)}{\pi_0(u_0 + 2\gamma_0 e^{kd/F_d})}\right] \tag{31}$$

$$\phi = \frac{u_0 + \pi_0 + \gamma_0 - u_0 x_2'}{\pi_0\sqrt{B'^2 - 4A'C'}}\left[\frac{\gamma_0\left[u_0\left(1 - \frac{kd}{2F_s}\right) + 2\gamma_0\right]}{\pi_0 x_2'} - \frac{\gamma_0 u_0^2\left(1 - \frac{kd}{2F_s}\right)}{\pi_0(u_0 + 2\gamma_0 e^{kd/F_d})}\right] \tag{32}$$

$$A' = A(s=0) = \frac{u_0^3\left(1 - \frac{kd}{2F_s}\right)}{\pi_0(u_0 + 2\gamma_0 e^{kd/F_d})} \tag{33}$$

$$B' = B(s=0) = \left\{u_0\left[u_0\left(1 - \frac{kd}{2F_s}\right) + 2\gamma_0\right](u_0 + 2\gamma_0 e^{kd/F_d}) + u_0^2\left(1 - \frac{kd}{2F_s}\right)(u_0 + \gamma_0 + \pi_0) + u_0\gamma_0\pi_0\left(1 - \frac{kd}{2F_s}\right)e^{kd/F_d}\right\} / \{\pi_0(u_0 + 2\gamma_0 e^{kd/F_d})\} \tag{34}$$

$$C' = C(s=0) = \frac{\left[u_0\left(1 - \frac{kd}{2F_s}\right) + 2\gamma_0\right](u_0 + \pi_0 + \gamma_0)}{\pi_0} - \frac{u_0\gamma_0\left(1 - \frac{kd}{2F_s}\right)e^{kd/F_d}}{(u_0 + 2\gamma_0 e^{kd/F_d})} - 2\gamma_0 \tag{35}$$

$$x_{1,2}' = x_{1,2}(s=0) = \frac{B' \pm \sqrt{(B'^2 - 4A'C')}}{2A'} \tag{36}$$

Equations 30−36 can now be utilized to calculate the run length distribution of two coupled motor proteins.

Analyzing our model, we conclude that the collective dynamics of two coupled molecular motors is determined by seven parameters: the step size, the forward rate, the detachment rate, the rebinding rate, the stall force, the detachment force, and the spring constant between the two motor proteins. For convenience, we collected all these parameters and their specific values for kinesin motor proteins in Table 1.

Quantifying the Cooperativity for Two Motor Proteins. It is clear that the run length distribution of the motor protein assembly reflects the degree of cooperation between two motors. Our theoretical analysis allows us to develop a quantitative measure of such cooperativity for multiple-motor proteins. For this purpose, we introduce a new function, which describes the cumulative run length distribution

Table 1. Parameters Employed To Describe the Collective Dynamics of Two Coupled Kinesins[a]

d	8.2 nm
u_0	121.95 s^{-1}
γ_0	1.0 s^{-1}
π_0	5.0 s^{-1}
F_s	6.0 pN
F_d	3.0 pN
k	0.2 pN/nm

[a]We followed a previous work to determine the values of some parameters[24] but also used two additional parameters: the forward rate u_0 is scaled to be 121.95 s^{-1} so that the velocity of a single kinesin $V_0 = u_0 d$ is fixed to 1.0 μm/s, and the spring constant k is set to be 0.2 pN/nm to follow the estimation from a previous experimental study.[38].

$$S^{\text{two-motors}}(l) = \sum_{i \geq l}^{\infty} P(i) \tag{37}$$

It has a physical meaning of the probability to have the run length larger than the length l. From eq 30 we obtain

$$S^{\text{two-motors}}(l) = -\frac{\theta}{1 - 1/x_1'}(x_1')^{-l/d} + \frac{\phi}{1 - 1/x_2'}(x_2')^{-l/d} \tag{38}$$

Since $x_1' > x_2' > 1$, the first term in this equation will decay faster than the second term. Therefore, when l is large (processive motor proteins usually walk hundreds of steps before dissociation),[4] the cumulative run length distribution can be approximated by the second term

$$S^{\text{two-motors}}(l) \simeq \frac{\phi}{1 - 1/x_2'}(x_2')^{-l/d} = \frac{\phi}{1 - 1/x_2'}e^{-l/\lambda_2} \tag{39}$$

where $\lambda_2 = d/\ln[x_2']$. This result suggests that $S^{\text{two-motors}}(l)$ can be approximately described as an exponentially decaying function with a characteristic length scale λ_2. The same arguments for eq 30 for large l suggest that $P(l) \sim (x_2')^{-l/d} = e^{-l/\lambda_2}$. This means that λ_2 is also the mean run length of the two-motor complex, which is defined as $\langle l \rangle = \int_0^\infty lP(l)\,dl$ under these conditions.

To measure the cooperativity, the run length distributions for two-motors system must be compared with the run length distribution of a single motor at the same conditions. The explicit form for the cumulative run length distribution for a single motor can be derived from known results by setting the backward rate to zero.[15] We obtain the following expression in our notations

$$S^{\text{single-motor}}(l) = \frac{(\gamma_0 + u_0)^{-l/d}}{u_0} = e^{-l/\lambda_1} \tag{40}$$

with a characteristic length $\lambda_1 = d/\ln\left[\frac{(\gamma_0 + u_0)}{u_0}\right]$, which also can be shown as the mean run length of the single motors. Therefore, the ratio between the two cumulative run length distribution functions can be represented by an exponential function

$$R(l) = \frac{S^{\text{two-motors}}(l)}{S^{\text{single-motor}}(l)} = \frac{\phi}{1 - 1/x_2'}e^{cl/\lambda_2} \tag{41}$$

with a new dimensionless parameter c is defined as

DOI: 10.1021/acs.jpcb.9b04710
J. Phys. Chem. B 2019, 123, 5805−5813

$$c = \frac{\lambda_2 - \lambda_1}{\lambda_1} \tag{42}$$

It describes the relative increase in the mean run length for the two-motor system in comparison with the single-motor case at the same conditions. For this reason, the parameter c is a convenient measure of the cooperativity. The larger c, the more cooperative is the multimotor complex.

RESULTS

Application of Theoretical Analysis for Kinesin Motor Proteins. Let us apply our theoretical approach to investigate the run length distributions and the degree of cooperativity for the system of two coupled kinesin-1 proteins that move along microtubule filaments. These motors are currently the most investigated, and the dynamic properties of this system are well described.[31] The run length distribution and the cumulative run length distribution are calculated by using eqs 30 and 38, respectively. All parameters needed for calculations are known,[16] and they are presented in Table 1. In addition, to test our theoretical predictions, we performed Monte Carlo computer simulations of the system by employing the Gillespie algorithm and comparing the results with those from the analytical calculations. Recall that in the analytical calculations the assumption that leading and trailing motors alternate was made. However, this condition was removed for Monte Carlo computer simulations. In computer simulations moving motors were chosen randomly (not alternating), and the distance more than two sites between proteins was allowed.

The results of theoretical calculations and computer simulations are presented in Figure 2. First, one can see that theoretical predictions perfectly agree with Monte Carlo simulations, suggesting that our alternation assumption for leading and trailing motors is reasonable, and it does not affect the dynamic description of the system for the realistic set of parameters given in Table 1. We predict also that the run length distribution of the single kinesin is a monotonically decreasing function of l (Figure 2A). This can be easily understood by noting that the longer motor stays on the linear track, the larger is the probability to dissociate. However, surprisingly, for the two-motors case, our method predicts a nonmonotonic run length distribution, as shown in Figure 2A. This can be explained by the fact that the two-motor complex dissociates from the filament only after both motors detach, but this does not happen simultaneously and it will take some time. Thus, the probability of very short runs for the two-motor complex should be low. The probability of having run lengths larger than $l \simeq 1$ μm is always larger for two-motor complexes (see Figure 2A).

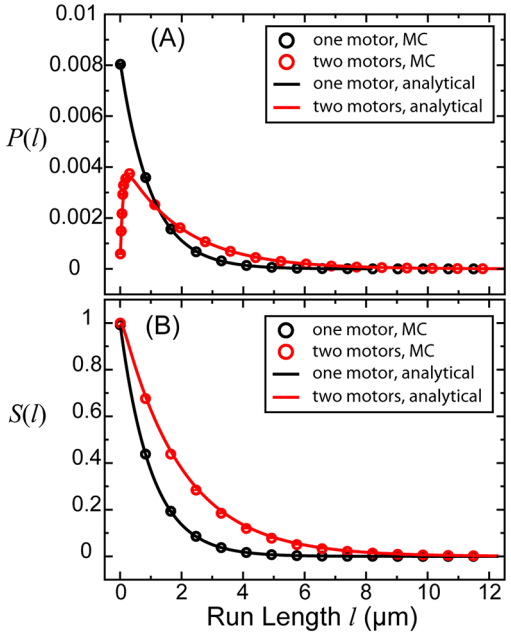

Figure 2. (A) Run length distribution of two coupled kinesins versus a single kinesin. (B) Cumulative run length distribution of two coupled kinesins versus a single kinesin. $S(l)$ represents the probability to have a run length of l or larger. Solid lines represent analytic calculation while open circles represent results from Monte Carlo simulations by using the Gillespie algorithm. Error bars are smaller than the circle size. The parameters are shown in Table 1.

Our results show that two coupled kinesins can significantly improve the transport efficiency compared to a single kinesin. The mean value of the run length $\langle l \rangle$ has a twofold increase from 1.0 μm for a single kinesin while it is equal to 2.0 μm for two coupled kinesins. This result is expected based on the fact that the probability of dissociating of two motors is significantly lower than that for the single-motor case. However, we emphasize here that the advantage for the cellular cargo to be moved by two motors versus a single motor includes not only a moderate increase in the mean run length but also a significant improvement for the long distances. For example, for a single kinesin the probability of having a run length larger than 6 μm is only 0.2%, while for the two coupled kinesins this probability gains a 20-fold increase to 4.9% (see Figure 2B). In fact, as shown in eq 41, the ratio between the cumulative run length distributions of the two coupled kinesins and the single kinesin is not a constant, and it increases exponentially with the run length.

Furthermore, to quantify the cooperativity of two coupled kinesin motor proteins, we estimated the dimensionless parameter c. For the set of parameters given in Table 1, it is found that $c \simeq 0.95$. This suggests that two coupled kinesin motors cooperate strongly enough, at least, from the point of view of increasing run lengths. Note, however, that the level of cooperativity might be different for other dynamics properties such as velocities and diffusion coefficients.[16] In addition, in our model the motor proteins are close to each in the two-motor bound conformations due to alternation assumption, and this might also artificially increase the degree of cooperativity.[16]

Factors Influencing the Degree of Cooperativity between Two Coupled Motor Proteins. Our theoretical method allows us to evaluate factors that influence the degree of cooperativity for two coupled motor proteins. More specifically, using the parameters for kinesin motor proteins, we analyze how changing the stepping rates, the motor dissociation equilibrium constants, and the spring constants affects the cooperativity parameter c, and the results are presented in Figure 3. First, stepping rates are varied from 30 to 200 nm/s. While the effect of increasing the stepping rate on the run length distribution is significant by making them less sharp (Figure 3A), the cooperativity parameter c is barely affected: Figure 3B shows the increase in c of only 0.01 while the stepping rate increases ~7 times.

At the same time, the dissociation properties of motor proteins influence the degree of cooperativity much stronger, as shown in Figures 3C and 3D. We define an equilibrium dissociation constant for a single-motor protein as $K_D = \gamma_0/\pi_0$, which describes the tendency of the molecule to dissociate from

DOI: 10.1021/acs.jpcb.9b04710
J. Phys. Chem. B 2019, 123, 5805−5813

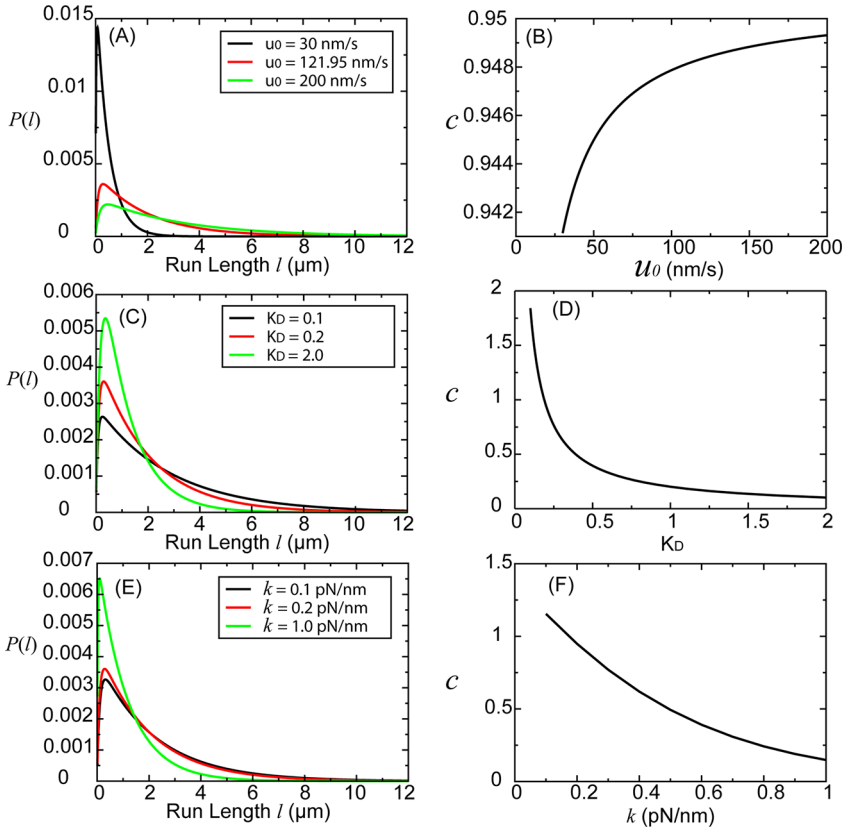

Figure 3. Cooperativity between two coupled motor proteins. (A) Run length distribution of two motors with different forward stepping rates. (B) c, defined as the relative increase in the mean run length for the two coupled motors versus the single motor case at the same condition, as a function of the forward stepping rate. (C) Run length distribution of two motors with different dissociation constants. (D) c as a function of the dissociation constant. (E) Run length distribution of two motors with different elastic spring constant between the two motors. (F) c as a function of the elastic spring constant between the two motors. The parameters are shown in Table 1.

the filament. The larger K_D, the larger is the probability for the motor to dissociate from the linear track. Increasing the dissociation constant makes the run length distributions sharper with decreasing mean run length: see Figure 3C. But the degree of cooperativity drops sharply (Figure 3D). This is because the time intervals after the first motor dissociation and before the second motor dissociation are getting smaller, decreasing the effect of the second motor on the run lengths.

The strength of intermolecular interactions also has a significant effect on the degree of cooperativity, as illustrated in Figures 3E and 3F. Increasing the spring constant makes these interactions stronger, and the run length distributions become more narrow; see Figure 3E. But this decreases the cooperativity parameter c. This observation can be explained by noting that the dissociation rate increases for larger spring constants (see eq 3), while the stepping rate decreases due to stronger intermolecular tension. Both of these factors lead to lower cooperativity in the system of two coupled motor proteins. This also agrees with predictions from a previous study that suggests that increasing the coupling will lead to run length reduction.[26]

Other important parameters that influence the dynamics of single-motor proteins are the stall force F_s, which specifies the external force that is needed to stop the forward motion of the motor, and the detachment force F_d, which specifies the characteristic force needed to detach the motor from the filament. Our analytical framework allows us to evaluate the effect of these quantities on the degree of cooperativity. The results are presented in Figure 4. Two qualitatively different

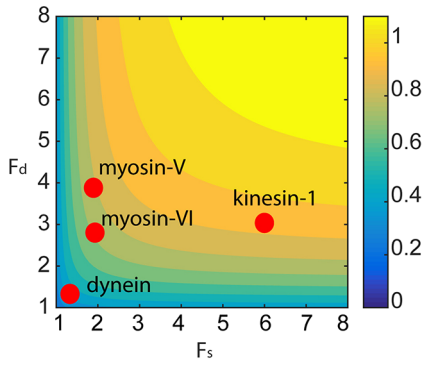

Figure 4. Cooperativity between two coupled motor proteins, quantified by c, defined as the relative increase in the mean run length for the two coupled motors versus the single-motor case at the same condition, as a function of the stalling force F_s and detachment force F_d (pN).

dynamic behaviors are observed. For large F_s and F_d, strong cooperativity is predicted (yellow-orange regions in Figure 4). In this case, the intermolecular interactions weakly influence the forward stepping motion, and the dissociations are rare. In the limit when the stalling and/or the dissociation forces are weak, the cooperativity is low (blue-green regions in Figure 4). In this situation, the motor cannot step forward (F_s is small) or it dissociates too quickly (F_d is small), leading to the decreased level of cooperativity.

DOI: 10.1021/acs.jpcb.9b04710
J. Phys. Chem. B 2019, 123, 5805−5813

Stall forces and dissociation forces are known for different motor proteins, and it is interesting then to use our analysis to determine the degree of cooperativity for each of the system. We checked four different motors: kinesin-1 (F_s = 6pN[24] and F_d = 3pN[24]), myosin V (F_s = 2pN[32] and F_d = 4pN[33]), myosin VI (F_s = 2pN[34] and F_d = 2.6pN[33]), and dynein (F_s = 1pN[35] and F_d = 1pN[24]). It is found that kinesins exhibit a high cooperativity (large c), while dyneins have a low cooperativity (small c); see Figure 4. Myosins V and myosins VI motor proteins show intermediate values of the parameter c. This suggests that processive motor proteins like kinesins might work together to increase their transport efficiency. In contrast, dyneins cannot make their cellular transport very efficient even by recruiting several copies of molecular motors. Interestingly, this might be the reason why in cells dyneins always function with the assisting protein dynactin. This increases the effective F_d for the dynein–dynactin complex, and then coupling several motor protein complexes together will lead to more efficient cellular transport,[36] as predicted in Figure 4.

CONCLUSIONS

We developed a new theoretical framework to evaluate run length distributions of coupled molecular motors that move along linear filaments. Our approach is based on first-passage explicit calculations, which are also tested by extensive Monte Carlo computer simulations. Specifically, we investigated dynamic properties of two coupled motor proteins. Our calculations show that the two coupled motors have a surprisingly nonmonotonic run length distribution as a function of the length, which differs from the monotonically decaying function for the single-motor protein molecules. These observations are explained by noting that two motors cannot simultaneously dissociate from the filament, leading to a more complex dynamic behavior for coupled motor protein systems. We also found that the transport efficiency of two interacting molecular motors is much higher in comparison with the single motors. The degree of cooperativity with respect to increasing run lengths is introduced and quantitatively described. The application of our method for two coupled kinesin motors proteins shows that these motors possess a strong ability to cooperate, although this might be the result of the assumption of the theoretical model that considers two-motor-bound conformations where motors are close to each other. Using our quantitative approach, the factors that affect the cooperativity are explicitly analyzed. It is shown that dissociation constants, strength of interactions, stall forces, and detachment forces strongly influence the degree of cooperativity, while the effect of stepping rates is minimal. Finally, our framework is utilized to evaluate the level of cooperativity with respect to increasing run lengths for different motor protein systems.

Although our theoretical method is able to clarify several aspects of the collective dynamics of motor proteins, it is important to critically evaluate our findings. There are several approximations which should limit the applicability of this approach. We do not take into account the backward transition rates for motor proteins, which violates the detailed balance condition. However, for most of motor proteins, the backward transition rates are small in the absence of external loads. Therefore, it is a safe approximation to study only the dynamical properties of motor proteins. But one should notice that under external loads some of these rates might become quite large. Thus, it is also thermodynamically inconsistent to neglect them.[4] Those effects will be considered in the future investigations. The unrealistic linear force/velocity relation is assumed for the stepping transition, while the susceptibility of motor velocities to the external forces, which depends on the functional form of the force–velocity relation, influences the collective dynamic behavior of motor proteins.[16,37] Another strong assumption is the alternation of the motion by leading and trailing motor proteins, which limits the number of possible molecular conformations. Our method also does not take into account the existence of intermediate chemical states and the finite length of linear filaments. However, despite these limitations, we believe that the method clarifies several physical–chemical aspects of the collective behavior of motor proteins, as indicated by our Monte Carlo computer simulations. It also provides a quantitative measure of the degree of cooperation and gives experimentally testable predictions.

AUTHOR INFORMATION

Corresponding Author

*E-mail: tolya@rice.edu.

ORCID

Anatoly B. Kolomeisky: 0000-0001-5677-6690

Notes

The authors declare no competing financial interest.

ACKNOWLEDGMENTS

The work was supported by the Welch Foundation (C-1559), by the NSF (CHE-1664218), and by the Center for Theoretical Biological Physics sponsored by the NSF (PHY-1427654).

REFERENCES

(1) Alberts, B.; Bray, D.; Hopkin, K.; Johnson, A. D.; Lewis, J.; Raff, M.; Roberts, K.; Walter, P. *Essential Cell Biology*; Garland Science: New York, 2015.

(2) Lodish, H.; Berk, A.; Darnell, J. E.; Kaiser, C. A.; Krieger, M.; Scott, M. P.; Bretscher, A.; Ploegh, H.; Matsudaira, P. *Molecular Cell Biology*; Macmillan: New York, 2008.

(3) Howard, J. *Mechanics of Motor Proteins and the Cytoskeleton*; Sinauer Associates: Sunderland, MA, 2001.

(4) Kolomeisky, A. B. *Motor Proteins and Molecular Motors*; CRC Press: Boca Raton, FL, 2015.

(5) Cross, R. A.; McAinsh, A. Prime Movers: the Mechanochemistry of Mitotic Kinesins. *Nat. Rev. Mol. Cell Biol.* **2014**, *15*, 257.

(6) Kolomeisky, A. B.; Fisher, M. E. Molecular Motors: a Theorist's Perspective. *Annu. Rev. Phys. Chem.* **2007**, *58*, 675–695.

(7) Hancock, W. O. Bidirectional Cargo Transport: Moving beyond Tug of War. *Nat. Rev. Mol. Cell Biol.* **2014**, *15*, 615.

(8) Ebbing, B.; Mann, K.; Starosta, A.; Jaud, J.; Schols, L.; Schule, R.; Woehlke, G. Effect of Spastic Paraplegia Mutations in KIF5A Kinesin on Transport Activity. *Hum. Mol. Genet.* **2008**, *17*, 1245–1252.

(9) Hanemann, C.; Ludolph, A. Motor Protein Diseases of the Nervous System. *Amyotrophic Lateral Scler.* **2005**, *6*, 197–201.

(10) Hirokawa, N. Kinesin and Dynein Superfamily Proteins and the Mechanism of Organelle Transport. *Science* **1998**, *279*, 519–526.

(11) Veigel, C.; Schmidt, C. Moving into the Cell: Single-molecule Studies of Molecular Motors in Complex Environments. *Nat. Rev. Mol. Cell Biol.* **2011**, *12*, 163–176.

(12) Walter, W.; Beranek, V.; Fischermeier, E.; Diez, S. Tubulin Acetylation Alone Does Not Affect Kinesin-1 Velocity and Run Length in Vitro. *PLoS One* **2012**, *7*, e42218.

(13) Reck-Peterson, S.; Yildiz, A.; Carter, A.; Gennerich, A.; Zhang, N.; Vale, R. Single-molecule Analysis of Dynein Processivity and Stepping Behavior. *Cell* **2006**, *126*, 335–348.

(14) Vu, H.; Chakrabarti, S.; Hinczewski, M.; Thirumalai, D. Discrete Step Sizes of Molecular Motors Lead to Bimodal Non-Gaussian Velocity Distributions under Force. *Phys. Rev. Lett.* **2016**, *117*, 078101.

DOI: 10.1021/acs.jpcb.9b04710
J. Phys. Chem. B 2019, 123, 5805–5813

(15) Zhang, Y.; Kolomeisky, A. Theoretical Investigation of Distributions of Run Lengths for Biological Molecular Motors. *J. Phys. Chem. B* **2018**, *122*, 3272−3279.
(16) McLaughlin, T.; Diehl, M. R.; Kolomeisky, A. B. Collective Dynamics of Processive Cytoskeletal Motors. *Soft Matter* **2016**, *12*, 14−21.
(17) Holzbaur, E.; Goldman, Y. Coordination of Molecular Motors: from in Vitro Assays to Intracellular Dynamics. *Curr. Opin. Cell Biol.* **2010**, *22*, 4−13.
(18) Klumpp, S.; Keller, C.; Berger, F.; Lipowsky, R. *Multiscale Modeling in Biomechanics and Mechanobiology*; Springer: London, 2015; pp 27−61.
(19) Vershinin, M.; Carter, B.; Razafsky, D.; King, S.; Gross, S. Multiple-motor Based Transport and Its Regulation by Tau. *Proc. Natl. Acad. Sci. U. S. A.* **2007**, *104*, 87−92.
(20) Furuta, K.; Furuta, A.; Toyoshima, Y.; Amino, M.; Oiwa, K.; Kojima, H. Measuring Collective Transport by Defined Numbers of Processive and Nonprocessive Kinesin Motors. *Proc. Natl. Acad. Sci. U. S. A.* **2013**, *110*, 501−506.
(21) Jamison, D.; Driver, J.; Rogers, A.; Constantinou, P.; Diehl, M. Two Kinesins Transport Cargo Primarily via the Action of One Motor: Implications for Intracellular Transport. *Biophys. J.* **2010**, *99*, 2967−2977.
(22) Driver, J.; Jamison, D.; Uppulury, K.; Rogers, A.; Kolomeisky, A.; Diehl, M. Productive Cooperation among Processive Motors Depends Inversely on Their Mechanochemical Efficiency. *Biophys. J.* **2011**, *101*, 386−395.
(23) Fisher, M.; Kolomeisky, A. Simple Mechanochemistry Describes the Dynamics of Kinesin Molecules. *Proc. Natl. Acad. Sci. U. S. A.* **2001**, *98*, 7748−7753.
(24) Muller, M.; Klumpp, S.; Lipowsky, R. Tug-of-war as a Cooperative Mechanism for Bidirectional Cargo Transport by Molecular Motors. *Proc. Natl. Acad. Sci. U. S. A.* **2008**, *105*, 4609−4614.
(25) Klumpp, S.; Lipowsky, R. Cooperative Cargo Transport by Several Molecular Motors. *Proc. Natl. Acad. Sci. U. S. A.* **2005**, *102*, 17284−17289.
(26) Berger, F.; Keller, C.; Klumpp, S.; Lipowsky, R. Distinct Transport Regimes for Two Elastically Coupled Molecular Motors. *Phys. Rev. Lett.* **2012**, *108*, 208101.
(27) Shao, Q.; Gao, Y. On the Hand-over-hand Mechanism of Kinesin. *Proc. Natl. Acad. Sci. U. S. A.* **2006**, *103*, 8072−8077.
(28) Bhabha, G.; Johnson, G.; Schroeder, C.; Vale, R. How Dynein Moves Along Microtubules. *Trends Biochem. Sci.* **2016**, *41*, 94−105.
(29) Valentine, M.; Fordyce, P.; Block, S. Eg5 Steps It Up! *Cell Div.* **2006**, *1*, 31.
(30) Block, S.; Asbury, C.; Shaevitz, J.; Lang, M. Probing the Kinesin Reaction Cycle with a 2D Optical Force Clamp. *Proc. Natl. Acad. Sci. U. S. A.* **2003**, *100*, 2351−2356.
(31) Wang, W.; Cao, L.; Wang, C.; Gigant, B.; Knossow, M. Kinesin, 30 Years Later: Recent Insights from Structural Studies. *Protein Sci.* **2015**, *24*, 1047−1056.
(32) Cappello, G.; Pierobon, P.; Symonds, C.; Busoni, L.; Gebhardt, J.; Rief, M.; Prost, J.; Christof, J. Myosin V Stepping Mechanism. *Proc. Natl. Acad. Sci. U. S. A.* **2007**, *104*, 15328−15333.
(33) Oguchi, Y.; Mikhailenko, S.; Ohki, T.; Olivares, A.; De La Cruz, E.; Ishiwata, S. Load-dependent ADP Binding to Myosins V and VI: Implications for Subunit Coordination and Function. *Proc. Natl. Acad. Sci. U. S. A.* **2008**, *105*, 7714−7719.
(34) Nishikawa, S.; Homma, K.; Komori, Y.; Iwaki, M.; Wazawa, T.; Hikikoshi Iwone, A.; Saito, J.; Ikebe, R.; Katayama, E.; Yanagida, T.; Ikebe, M. Class VI Myosin Moves Processively along Actin Filaments Backward with Large Steps. *Biochem. Biophys. Res. Commun.* **2002**, *290*, 311−317.
(35) Mallik, R.; Carter, B.; Lex, S.; King, S.; Gross, S. Cytoplasmic Dynein Functions as a Gear in Response to Load. *Nature* **2004**, *427*, 649−652.
(36) King, S.; Schroer, T. Dynactin Increases the Processivity of the Cytoplasmic Dynein Motor. *Nat. Cell Biol.* **2000**, *2*, 20−24.
(37) Wang, Q.; Diehl, M. R.; Jana, B.; Cheung, M. S.; Kolomeisky, A. B.; Onuchic, J. N. Molecular Origin of the Weak Susceptibility of Kinesin Velocity to Loads and Its Relation to the Collective Behavior of Kinesins. *Proc. Natl. Acad. Sci. U. S. A.* **2017**, *114*, E8611−E8617.
(38) Meyhofer, E.; Howard, J. The Force Generated by a Single Kinesin Molecule Against an Elastic Load. *Proc. Natl. Acad. Sci. U. S. A.* **1995**, *92*, 574−578.

DOI: 10.1021/acs.jpcb.9b04710
J. Phys. Chem. B 2019, 123, 5805−5813